

Impact Factor:

ISRA (India) = 6.317
ISI (Dubai, UAE) = 1.582
GIF (Australia) = 0.564
JIF = 1.500

SIS (USA) = 0.912
ПИИИ (Russia) = 3.939
ESJI (KZ) = 8.771
SJIF (Morocco) = 7.184

ICV (Poland) = 6.630
PIF (India) = 1.940
IBI (India) = 4.260
OAJI (USA) = 0.350

SOI: [1.1/TAS](#) DOI: [10.15863/TAS](#)

International Scientific Journal Theoretical & Applied Science

p-ISSN: 2308-4944 (print) e-ISSN: 2409-0085 (online)

Year: 2023 Issue: 11 Volume: 127

Published: 30.11.2023 <http://T-Science.org>

Issue



Article



Safar Khodjiev

Bukhara state university

Professor

safar1951@mail.ru

Utkir Jamolov

Bukhara state university

Master's student

jamolovutkir2001@gmail.com

MODELING AND NUMERICAL RESULTS OF INVESTIGATION OF THE INFLUENCE OF THE IRREGULARITY OF WAKE JETS ON MIXING IN FLAT CHANNELS

Abstract: In this work, based on the complete Navier-Stokes equations, numerical simulation of a compressible gas in flat channels of constant cross section is performed. For the convenience of solving the system of equations, the procedure of "dimensionless" coordinates and physical parameters was carried out, and the coordinate transformation transforming the rectangular computational domain into a square one, as well as the coordinate transformations that ensure the finite-difference grid thickening in areas with the sharpest change in the flow parameters, both in the inlet part and at the channel wall.

On the basis of the developed calculation algorithm, the influence of the non-design of coaxial jets on mixing and propagation in a limited flat channel was numerically studied.

Numerically identified and analyzed, what are the ratios of the height of the inlet slots, and the initial data on the temperature, velocity and pressure of the wake jets, which in the initial sections of the channel are observed (not observed) the recirculation zone.

Key words: internal flows, simulation, flow, numerical solution, pressure, jet, Navies-Stokes, coaxial, mixing, off-design.

Language: English

Citation: Khodjiev, S., & Jamolov, U. (2023). Modeling and numerical results of investigation of the influence of the irregularity of wake jets on mixing in flat channels. *ISJ Theoretical & Applied Science*, 11 (127), 347-355.

Soi: <http://s-o-i.org/1.1/TAS-11-127-43> **Doi:**  <https://dx.doi.org/10.15863/TAS.2023.11.127.43>

Scopus ASCC: 2200.

Introduction

The advent of modern high-speed computing tools make it possible to consider the numerical simulation of complex jet flows by solving exact equations expressing conservation laws.

Of great practical interest is the study of the influence of the initial data and the geometry of coaxial jets on mixing and propagation in a limited flat channel, since such flows are used in the creation of mixing and furnace devices, internal combustion engines, chemical and oil-gas industries.

Field experimental studies of the mixing of coaxial gas jets with different pressures, temperatures,

velocities and geometries, as well as other parameters in channels of constant and variable cross-sections, are in many cases difficult and analytical solutions are not always possible, therefore, to solve such problems, mathematical modeling methods using numerical methods.

Such flows in the channels can be accompanied by separations, motion of waves in the jet contact zone, recirculation zones and other complex processes that cannot be solved by the parabolized Navier-Stokes equations, although the solution of which is much simpler than integrating the original Navier-Stokes equations. Numerical modeling of viscous gas flows

Impact Factor:

ISRA (India) = 6.317
 ISI (Dubai, UAE) = 1.582
 GIF (Australia) = 0.564
 JIF = 1.500

SIS (USA) = 0.912
 ПИИИ (Russia) = 3.939
 ESJI (KZ) = 8.771
 SJIF (Morocco) = 7.184

ICV (Poland) = 6.630
 PIF (India) = 1.940
 IBI (India) = 4.260
 OAJI (USA) = 0.350

based on the complete Navier-Stokes equations is difficult, however, it gives exact solutions to the above flow cases [1-3].

The purpose of the work is to investigate the effects of the non-design of cocurrent flows on their mixing and propagation in flat channels on the basis of an effective computational algorithm for solving the complete Navier-Stokes equations for a viscous gas, and the little-studied region of parameters is of particular interest, when a recirculation flow zone is formed as a result of the interaction of jets. Few experimental studies of turbulent mixing of gas jets with different densities were studied in [4–8], concurrent flows in a channel of constant cross section in the presence of recirculation zones and the conditions for the formation of recirculation zones were studied in a number of works [9–12], but the relations areas (heights) of the cross section and pressure of flows at the inlet to the channel.

Numerous works are devoted to modeling and numerical studies of internal flows and mixing of flows in channels based on approximate and complete Navier-Stokes equations [1,2,13-17]. It is known that a complete picture of the flow can be obtained with complex internal flows, the numerical solution of the complete Navier-Stokes equations when modeling two-dimensional flows of a viscous compressible fluid. A more detailed review of methods and schemes for solving the Navier-Stokes equations is given in [18-21], and for calculating internal flows, an excellent systematic review is given in [1, 17].

Below, we describe the results of a numerical study of the influence of the non-design of coaxial flows on the mixing and propagation parameters of flows in a channel of constant cross section based on the full Navier-Stokes equations, with the cross-sectional areas of the flows at the inlet having different finite ratios.

Problem statements. Given a flat channel of length L height $2f_0$. The flow diagram is shown in fig. 1. Suppose the channel and the flow are symmetrical about the OX axis, the OY axis coincides with the inlet section of the channel, and the origin of coordinates is located on the axis of symmetry. At the entrance to the channel there are two jets I - near-wall and II - central (main), respectively, with their physical and geometric characteristics.

It was said above that the main goal of this work is the numerical study of the mixing and flow of turbulent gas jets in a channel of constant cross section, in the presence of specific factors, such as the occurrence of recirculation zones and shock waves in particular. In these cases, it is necessary to use the full уравнений Навье – Стокса.

To describe the flow, two-dimensional complete non-stationary Navier-Stokes equations are used, in a vector-conservative form [22-23]

$$\frac{\partial U}{\partial t} + \frac{\partial F(U)}{\partial x} + \frac{\partial G(U)}{\partial y} = \frac{\partial v_1(U, U_y)}{\partial x} +$$

$$+ \frac{\partial v_2(U, U_y)}{\partial x} + \frac{\partial W_1(U, U_x)}{\partial y} + \frac{\partial W_2(U, U_y)}{\partial y} \quad (1)$$

Relationship of total specific energy with internal and kinetic energy:

$$E = \rho C_\theta T + \frac{1}{2} \rho (u^2 + \vartheta^2). \quad (2)$$

State equation:

$$p = \rho T. \quad (3)$$

Expression for effective viscosity:

$$\mu = \mu_l + \mu_t, \quad (4)$$

where μ_l -laminar, μ_t -turbulent viscosity, U -vector of conservative variables; F, G, V_1, V_2, W_1, W_2 are flow vectors that look like:

$$U = \begin{bmatrix} \varphi_x & F_y & \rho & u \\ \varphi_x & F_y & \rho & u \\ \varphi_x & F_y & \rho & \vartheta \\ \varphi_x & F_y & E & \end{bmatrix} = \begin{bmatrix} \bar{\rho} \\ \bar{\rho} u \\ \bar{\rho} \vartheta \\ \bar{E} \end{bmatrix} = \begin{bmatrix} \rho \\ m \\ n \\ E \end{bmatrix};$$

$$F = \frac{1}{L \varphi_x} \begin{bmatrix} m \\ \frac{m^2}{\rho} + p \\ mn \\ \frac{m}{\rho} \\ \frac{m(E+p)}{\rho} \end{bmatrix}; \quad G = \begin{bmatrix} n \\ \Omega_1 m \\ \Omega_1 n + p \\ \Omega_1 (E+p) \end{bmatrix}.$$

$$W_1(U, U_x) = \frac{1}{ReL} \begin{bmatrix} 0 \\ N_x \\ -\frac{2}{3} M_x \\ \frac{(mN_x - \frac{2}{3} nM_x)}{\rho} \end{bmatrix},$$

$$W_2(U, U_y) = \frac{\varphi_x}{ReF_y} \begin{bmatrix} 0 \\ M_y \\ \frac{4}{3} N_y \\ \frac{\frac{4}{3} nN_y + (m+n)M_y}{\rho} + P_T T_y \end{bmatrix}$$

$$V_1(U, U_x) = \frac{F_y}{ReL^2 \varphi_x} \begin{bmatrix} 0 \\ \frac{4}{3} M_x \\ N_x \\ \frac{nN_x}{\rho} + \frac{4}{3} \frac{mM_x}{\rho} + P_T T_x \end{bmatrix},$$

$$V_2(U, U_y) = \frac{1}{ReL} \begin{bmatrix} 0 \\ -\frac{2}{3} N_y \\ M_y \\ \Omega_1 M_y + \left(-\frac{2}{3} m\right) \frac{N_y}{\rho} \end{bmatrix},$$

Impact Factor:

ISRA (India) = 6.317
 ISI (Dubai, UAE) = 1.582
 GIF (Australia) = 0.564
 JIF = 1.500

SIS (USA) = 0.912
 ПИИЦ (Russia) = 3.939
 ESJI (KZ) = 8.771
 SJIF (Morocco) = 7.184

ICV (Poland) = 6.630
 PIF (India) = 1.940
 IBI (India) = 4.260
 OAJI (USA) = 0.350

$$W_2(U, U_y) = \frac{\varphi_x}{ReF_y} \left[\begin{array}{c} 0 \\ M_y \\ \frac{4}{3}N_y \\ \frac{4}{3}nN_y + (m+n)M_y \\ \rho \end{array} \right] + P_T T_y$$

$$\text{where } M_x = \frac{\mu(m_x\rho - \rho_x m)}{\rho^2}, M_y = \frac{\mu(m_y\rho - \rho_y m)}{\rho^2},$$

$$N_x = \frac{\mu(n_x\rho - \rho_x n)}{\rho^2}, N_y = \frac{\mu(n_y\rho - \rho_y n)}{\rho^2},$$

$$P_T = \frac{C_p\mu}{Pr_T}, \Omega_1 = \frac{n}{\rho}, Re = \frac{\rho_2 u_2 f_0}{\mu_2}$$

The system of equations (1-4), for the convenience of the numerical solution, is written in a dimensionless form for the channel in a reduced square form, and by introducing the function F(y) it allows to condense the design points near the wall in the physical plane while maintaining a constant step in the design plane and the function $\varphi(x)$ crowding calculated points in the inlet part of the channel [22].

Dimensionless quantities are associated with dimensional relationships in the form

$$\bar{x} = \frac{x}{f_0}; \bar{y} = \frac{y}{f_0}; \bar{u} = \frac{u}{u_2}; \bar{\vartheta} = \frac{\vartheta}{u_2}; \bar{E} = \frac{E}{\rho_2 u_2^2};$$

$$\bar{p} = \frac{p}{\rho_2 u_2^2};$$

$$\bar{\mu} = \frac{\mu}{\rho_2 f_0 u_2}; \bar{t} = \frac{t}{\frac{f_0}{u_2}}; \bar{\rho} = \frac{\rho}{\rho_2}; \bar{T} = \frac{T}{\frac{u_2^2}{R_m}}; \bar{C}_p = \frac{C_p}{R_m};$$

$$\bar{C}_\vartheta = \frac{C_\vartheta}{R_m}; \bar{L} = \frac{L}{f_0}; Re = \rho_2 f_0 u_2 / \mu_2. \quad (5)$$

Index 2 denotes the values of the parameters of the central jet at the channel inlet. The transition from a rectangular channel to a square one was carried out by transforming the coordinates: $\xi = \bar{x}/\bar{L}$, $\eta = \bar{y}$.

Boundary and initial conditions. The solution of the problem posed is found for stationary boundary conditions and, starting from the problem statement, can have the following form:

$$t = t_0;$$

$$x = 0:$$

$$u = u_2, \vartheta = 0, E = E_2, \mu = \mu_2, \rho = \rho_2, p = p_2,$$

when $0 \leq y \leq R_2$,

$$u = u_1, \vartheta = 0, E = E_1, \mu = \mu_1, \rho = \rho_1, p = p_1,$$

when $R_2 < y < 1$,

$$u = 0, \vartheta = 0, E = E_w, \mu = \mu_w, \rho = \rho_w, p = p_w,$$

when $y = 1$.

$$0 < x \leq 1:$$

$$u = 0, \vartheta = 0, E = E_0, \mu = \mu_0, \rho = \rho_0, p = p_0,$$

when $0 < y < 1$,

$$u = 0, \vartheta = 0, E = E_w, \mu = \mu_w, \rho = \rho_w, p = p_w,$$

when $y = 1$.

$t > t_0:$

$x = 0:$

$$u = u_2, \vartheta = 0, E = E_2, \mu = \mu_2, \rho = \rho_2, p = p_2,$$

when $0 \leq y \leq R_2$, (6)

$$u = u_1, \vartheta = 0, E = E_1, \mu = \mu_1, \rho = \rho_1, p = p_1,$$

when $R_2 < y < 1$, (7)

$$u = 0, \vartheta = 0, E = E_w, \mu = \mu_w, \rho = \rho_w, p = p_w,$$

when $y = 1$. (8)

$0 < x \leq 1:$

$$\left\{ \begin{array}{l} u = 0, \vartheta = 0, E = \tilde{E}_w \\ \rho = \tilde{\rho}_w, \frac{\partial P}{\partial y} = 0, \mu = \tilde{\mu}_w, T = \tilde{T}_w \end{array} \right\} \text{ when } y = 1 \quad (9)$$

$$\left\{ \begin{array}{l} \frac{\partial u}{\partial y} = \vartheta = \frac{\partial E}{\partial y} = 0 \end{array} \right\} \text{ when } y = 0. \quad (10)$$

$x = 1:$

$$\left\{ \frac{\partial u}{\partial x} = \frac{\partial \vartheta}{\partial x} = \frac{\partial E}{\partial x} = 0 \left(\text{or } \frac{\partial^2 u}{\partial x^2} = \frac{\partial^2 \vartheta}{\partial x^2} = \frac{\partial^2 E}{\partial x^2} \right), \right.$$

when $0 < y < 1$. (11)

Conditions (5-11) subscripts 1, 2, w-respectively refers to the parameters of the near-wall, central jet and on the wall, ρ_1, E_1, μ_1 and ρ_2, E_2, μ_2 , respectively, are calculated for a given temperature T_1, T_2 and pressure p_1, p_2 of the wall and central jet. The numerical values $\rho_w, E_w, \tilde{\rho}_w, \tilde{E}_w, \tilde{\mu}_w$ are calculated by setting the boundary conditions on the wall in terms of u, ϑ, T, P , and $u_0, E_0, \rho_0, \mu_0, T_0$ are some initial values of the required parameters. All of the above notation is generally accepted [3,22], and as usual, the x, y coordinates, as well as dimensionless variables, are written without an overline.

The given boundary conditions at the inlet ($x = 0$) correspond to the stepwise assignment of homogeneous gas flows in the inlet section of the channel. The flow is symmetrical with respect to the x axis, therefore, for the values $y = 0$ and $0 < x \leq 1$ the flow symmetry conditions are set. As the boundary conditions at the channel output at $x = 1$ relations are used that correspond to linear extrapolation of the desired u, ϑ, E variables over the internal nodes of the computational grid. The boundary conditions on the wall at $t = t_0$ and $t > t_0$ in terms of velocities were set to stationary conditions of sticking $u = 0$ and impermeability $\vartheta = 0$, and at $t = t_0$ in the case of setting T_w of the wall temperature, p_w are found from the equation of state.

Solution method. For the numerical solution of the system of equations (1-4) with boundary conditions (5-11), an effective implicit Beam-Warming finite-difference scheme was used for the numerical integration of the Navier-Stokes equations in the form of conservation laws for a compressible gas [23]. This scheme and algorithm is non-interactive and retains a conservative form, which is important for studying internal flows with a recirculation zone. In addition, the results of calculations [22, 23] show that the scheme has sufficient computational stability and accuracy for

Impact Factor:

ISRA (India) = 6.317
 ISI (Dubai, UAE) = 1.582
 GIF (Australia) = 0.564
 JIF = 1.500

SIS (USA) = 0.912
 ПИИИ (Russia) = 3.939
 ESJI (KZ) = 8.771
 SJIF (Morocco) = 7.184

ICV (Poland) = 6.630
 PIF (India) = 1.940
 IBI (India) = 4.260
 OAJI (USA) = 0.350

Courant numbers greater than one. When solving equation (1), a one-step finite-difference scheme was used in the form [23]

$$\Delta U^n = \frac{\theta \Delta t}{1 + \theta_2} \frac{\partial}{\partial t} \Delta U^n + \frac{\Delta t}{1 + \theta_2} \frac{\partial}{\partial t} U^n + \frac{\theta_2}{1 + \theta_2} \Delta U^{n-1} + 0 \left[\left(\theta - \frac{1}{2} - \theta_2 \right) \Delta t^2 + \Delta t^3 \right], \quad (12)$$

where $\Delta U^n = U^{n+1} - U^n$ and $U^n = U(n \Delta t)$ are solutions of the partial differential equation (1). The calculations were carried out at $\theta=1$ and $\theta_2=0.5$, which means that scheme (12) will be three-layer of the second order of accuracy. In addition, the delta form retains the advantageous property of a stationary state, if it exists, to be independent of the time step size [23].

To obtain a numerical solution, it is necessary to set the initial time $t = t_0$ of the gas-dynamic quantities, for example, as from condition (5). At the beginning of the calculation, at the boundaries and in all internal nodes, the viscosity was set depending on temperature in the form $\mu = \text{const} \cdot T^{0.6472}$. On the wall at pressure $t > t_0$, a much less stringent condition $\frac{\partial P}{\partial y} = 0$ is set, since the constancy of P is assumed only across the sublayer adjacent to the wall with a thickness equal to Δy .

As a method for numerically solving the problem, we used the algorithm described in [22], where the spatial derivatives were approximated by the second order of accuracy $O(\Delta x^2, \Delta y^2)$.

The effective turbulent viscosity is calculated using an algebraic model in the form

$$\mu = \text{const} T^{0.6472} + \chi \rho b^2(x) \left| \frac{\partial u}{\partial y} \right|, \quad (13)$$

here χ is the empirical turbulence constant, $b(x)$ is the conditional width of the mixing region;

Steady-state solutions are considered obtained if the conditions are met at all grid points

$$m \alpha x \left| \frac{\Delta U_{i,j}^n}{U_{i,j}^n \Delta t} \right| < \varepsilon \quad (14)$$

where ε is a small number, taken as options, equal to 0.0001.

Results of a numerical study. To study the patterns of propagation of cocurrent flows with different pressures in a channel of constant cross section, a channel was chosen, as in [11], with geometric data: $D=188$ mm ($f_0=0.94$ mm - half-height), $L=1.4$ m. Calculations assumed that both air flows, heat capacity at constant pressure and heat capacity at constant volume are constant, $Pr_T = Pr=0.7$. The main calculations were carried out under the condition on the wall along T in the form $\partial T / \partial y = 0$

The calculations performed for various initial data and their variants are shown in the table. The main

calculation results are presented in the form of graphs in Figs. 2.

The results of options № 1 and № 2, i.e. at the same temperatures of the jet and cocurrent $T_1 = T_2 = 300$ K ($\varphi_4 = 1$) as well as at $T_1 = 300$ K and $T_2 = 700$ K ($\varphi_4 = 2.333$) with the rest constant parameters, shows that in the second variant there are recirculation zones (reverse currents) in the initial sections of the channel. At the same temperatures of the jet and concurrent, this is not observed. Increasing the temperature of the jet promotes the development of the flow. In both cases, in the initial sections of the channel, the axial value of the longitudinal velocity first increases, and decreases with distance from the channel exit. This can be explained by the fact that an increase in temperature leads to an acceleration of the flow and a decrease in pressure in the initial sections.

Options № 3 and № 4 differ from the previous ones by the pressure of the jet and daily flow, which are respectively equal to 4 atm and 1 atm. In these options, similar flow patterns are also observed, an increase in the initial values of temperature and pressure to a jet of 4 atm leads to a sharp increase in the axial values of the longitudinal velocity in the initial sections of the channel, and when moving away from the channel exit, to its rapid drop. Such patterns were not observed in [11, 12].

On fig. 2 shows the transverse distributions of temperature and pressure at various distances from the channel exit (———— - option № 3, - - - - - option № 4). It can be noted here that, as the temperature and pressure move away from the inlet section of the channel, they equalize along the cross section and tend to a uniform value. The axial value of temperature and pressure is also given here. It can be seen from the graph that the axial value near the mouth of the slot first falls, in the recirculation zone it increases, and as the distance from the nozzle exit, the temperature decreases and tends to a constant value.

On fig. 3-6 show the results of the calculation for the case when the flow velocity is set to essentially subsonic along the central slot, and along the peripheral slot - sonic and supersonic. On fig. Figures 3-4 show the transverse and axial distributions of the longitudinal velocity and pressure, respectively, for options № 5 and № 6. Figure 3 shows the transverse distributions of the longitudinal velocity at different distances of the channel, as well as the axial change in the longitudinal velocity at $R_2/f_0 = 0.5$ (solid line), $R_2/f_0 = 0.26$ (dotted line). As follows from the graphs, as we move away from the channel exit, the velocity profile gradually smoothest out, the maximum velocity value tends to the jet axis, while taking on a parabolic form, the axial velocity value in the initial sections increases, and decreases as we move away from the beginning of the section.

On fig. 4 shows the transverse distribution and axial pressure change at slot ratios $R_2/f_0 = 0.5$ and $R_2/f_0 = 0.26$ (solid and dotted lines, respectively). As

Impact Factor:

ISRA (India)	= 6.317	SIS (USA)	= 0.912	ICV (Poland)	= 6.630
ISI (Dubai, UAE)	= 1.582	ПИИИ (Russia)	= 3.939	PIF (India)	= 1.940
GIF (Australia)	= 0.564	ESJI (KZ)	= 8.771	IBI (India)	= 4.260
JIF	= 1.500	SJIF (Morocco)	= 7.184	OAJI (USA)	= 0.350

can be seen from the graphs, with a small slot ratio, the transverse pressure distribution equalizes faster, and the axial value drops rapidly. This is obvious, since the flow flowing out of the smaller slot loses its momentum faster and equalizes with the flow flowing out of the larger slot. On fig. 5 and fig. Figure 6 shows the transverse distributions of the longitudinal velocity, pressure, as well as the axial change in velocity, temperature and pressure at the slot ratio $R_2/f_0 = 0,26$, while the more heated gas is supplied through the central slot (option №. 7).

Here it can be noted that the transverse distributions of the velocity and pressure profiles are similar to other cases, when the axial change in velocity in the initial sections increases rapidly, and with distance from the beginning it gradually decreases and tends to a constant value. This is explained by the fact that when mixing two viscous flows, where the speed of the larger one involves a flow with a lower speed, it thereby leads to an acceleration of the flow with a lower speed at the initial sections of the channel. The axial value of pressure increases in the initial sections, while the temperature decreases. This is due to the fact that, at the mixing boundary, the deceleration of the flow at a high speed leads to an increase in the pressure value, and the temperature drops, transferring heat from a more to a less heated flow.

Variants №. 8 and №. 9, at a heated temperature of the central jet and low pressure ratios of the jet and cocurrent flow ($P_2/P_1 = 1$), as well as two values of φ_2 in the mixing region, abrupt changes in the velocity and temperature profiles are not observed, and also in both cases the core and high temperature are maintained until the end of the channel.

The results of variant №. 10 showed that noticeable flow recirculation zones are traced in the initial sections, and when moving away, the transverse distribution of the longitudinal velocity passes to a parabolic profile. At $\bar{x} = 0.03, 0.07, 0.2, 0.4$, the height of the recirculation zone occupies, respectively, $0.64f_0, 0.48f_0, 0.35f_0, 0.10f_0$ of the channel section, and reaches half the channel length.

On fig. 7 shows the transverse distributions of the longitudinal velocity

(- · - option №11; ---- - option №.12; ——— - option №.13), as well as the axial value of the longitudinal velocity with different values of temperature and pressure. In all three variants, a recirculation zone is observed in the initial sections of the channels; reverse currents. At constant parameters $\varphi_1, \varphi_2, \varphi_3, \varphi_5$, an increase in the temperature of the main jet, respectively, leads to an expansion of the reverse flow region, and in these zones the transverse pressure change is harmonious. This phenomenon can

be explained by the fact that in the reverse flow zones, i.e. at the boundary of the mixing of two jets, the jet moving at a speed of about - and supersonic involves a jet moving at subsonic speed. In this case, a jet with a high speed loses part of its inertia due to deceleration, and a subsonic jet accelerates, naturally, in the mixing region, a decrease in the value of the jet velocity occurs, due to which a decrease in speed leads to an increase in pressure, and an increase in speed vice versa, which thereby leads to to a harmonious change in transverse pressure.

Numerical results showed that even at pressure ratio $P_2/P_1 = 1$, but at high temperature ratios ($T_2/T_1 = 2.3333$), a recirculation zone is also observed in the initial sections (option . 14, Fig. 8). On fig. Figure 8 shows the axial changes in the longitudinal velocity along the channel, as well as its transverse distributions in different sections of the channel. As follows from the graph, the axial value of the longitudinal velocity in the initial sections decreases, and as it moves away, it increases and tends to its constant value.

From the profiles of the transverse distributions of the longitudinal velocity, given in different sections of the channel, it follows that in the inlet sections near the channel wall, reverse current lines are traced, and as they move away, they extend and pass to a fully developed flow.

Conclusion.

The paper presents the results of a numerical study of the influence of the non-design of coaxial jets on mixing and propagation in a limited flat channel obtained by numerical solution of the non-stationary full Navier-Stokes equations by the method of implicit finite-spaced schemes. In particular, the following regularities were revealed:

- at different initial pressures and large ratios of jet velocities and temperatures, a recirculation zone is observed in the initial sections of the channel;
- at high ratios of initial pressure (4:1) and jet temperature, it leads to a sharp increase in the axial values of the longitudinal velocity in the initial sections of the channel;
- if the central jet is essentially subsonic and wall-mounted sonic or supersonic, in the initial sections there is no recirculation zone, and with a small ratio of slots, the pressure distribution levels out faster, and the axial value drops rapidly;
- at small ratios of velocity and heated temperature of the central jet and at small ratios of pressure of the jet and cocurrent ($P_2/P_1 = 1$), no sharp changes in the velocity and temperature profiles are observed, and the core and high temperature persist until the end of this channel.

Impact Factor:

ISRA (India) = 6.317	SIS (USA) = 0.912	ICV (Poland) = 6.630
ISI (Dubai, UAE) = 1.582	ПИИЦ (Russia) = 3.939	PIF (India) = 1.940
GIF (Australia) = 0.564	ESJI (KZ) = 8.771	IBI (India) = 4.260
JIF = 1.500	SJIF (Morocco) = 7.184	OAJI (USA) = 0.350

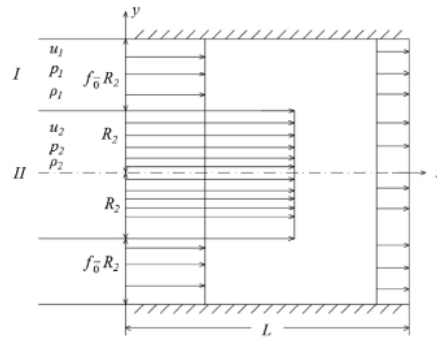


Fig 1. Scheme of the flow.

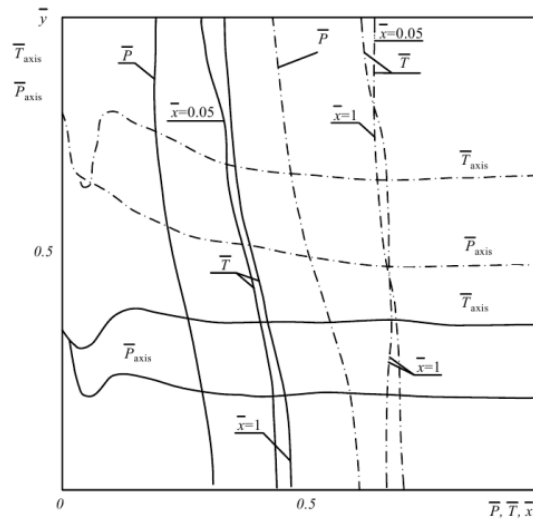


Fig. 2. Transverse changes in temperature and pressure at different distances from the inlet section of the channel, as well as their axial changes along the channel: — -option № 3; - · - option № 4.

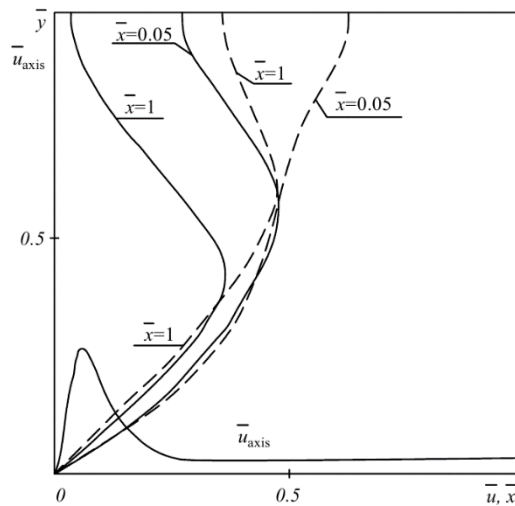


Fig 3. Transverse and axial distributions of longitudinal velocity: - - - option №. 5; — option №. 6.

Impact Factor:

ISRA (India) = 6.317	SIS (USA) = 0.912	ICV (Poland) = 6.630
ISI (Dubai, UAE) = 1.582	ПИИЦ (Russia) = 3.939	PIF (India) = 1.940
GIF (Australia) = 0.564	ESJI (KZ) = 8.771	IBI (India) = 4.260
JIF = 1.500	SJIF (Morocco) = 7.184	OAJI (USA) = 0.350

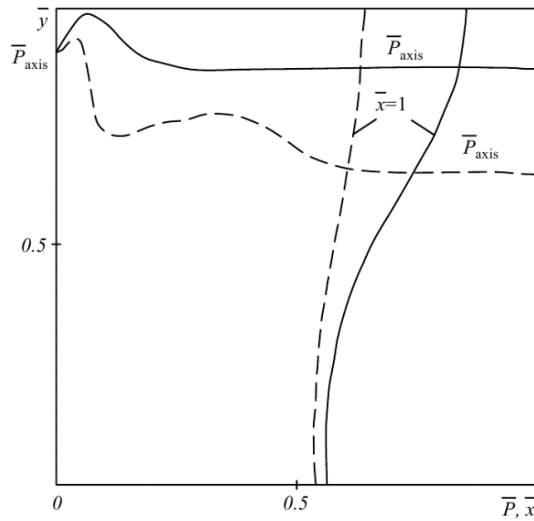


Fig 4. Transverse and axial pressure distributions:
 - - - option №. 5; ——— option №. 6.

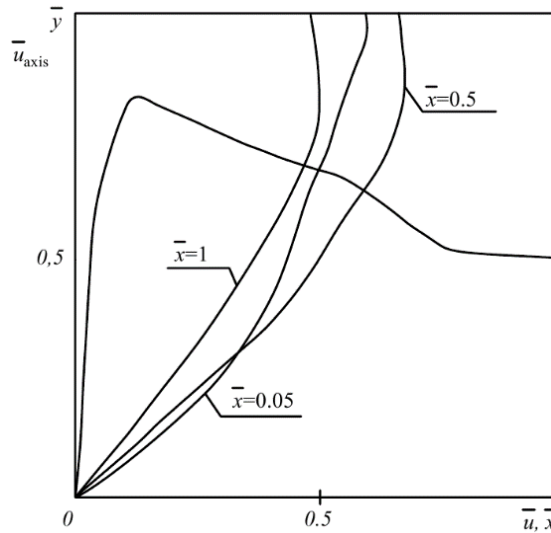


Fig 5. Transverse and axial distributions of longitudinal velocity: option №. 7.

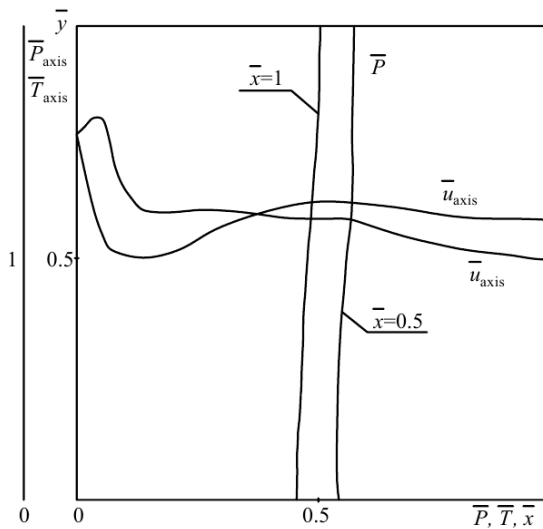


Fig 6. Transverse and axial change in temperature and pressure: option №. 7.

Impact Factor:

ISRA (India) = 6.317	SIS (USA) = 0.912	ICV (Poland) = 6.630
ISI (Dubai, UAE) = 1.582	ПИИИ (Russia) = 3.939	PIF (India) = 1.940
GIF (Australia) = 0.564	ESJI (KZ) = 8.771	IBI (India) = 4.260
JIF = 1.500	SJIF (Morocco) = 7.184	OAJI (USA) = 0.350

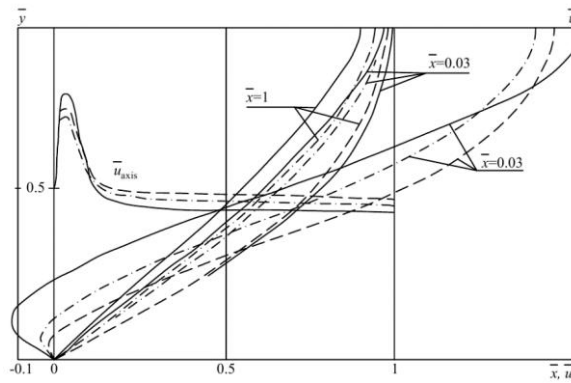


Fig 7. Transverse and axial change in longitudinal speed:
 - . . . - option №. 11; - - - - option №. 12; ——— - option №. 13.

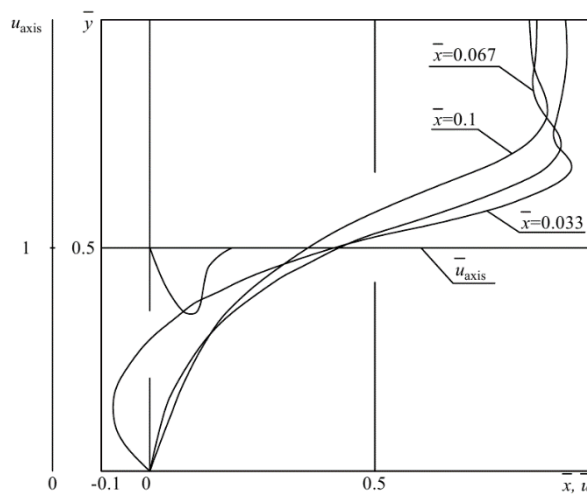


Fig 8. Transverse profiles of the longitudinal velocity in different sections of the channel, as well as its axial change along the channel: option №. 14.

Table 1.

N	$\varphi_1 = u_2/u_1$	$\varphi_2 = R_2/f_0$	$\varphi_3 = L/f_0$	$\varphi_4 = T_2/T_1$	$\varphi_5 = P_2/P_1$
1	72.4636	0,5	14.8936	1	2
2	72.4636	0,5	14.8936	2.3333	2
3	72.4636	0,5	14.8936	1	4
4	72.4636	0,5	14.8936	2.3333	4
5	0.02222	0,26	14.8936	1	2
6	0.02222	0,5	14.8936	1	2
7	0.02222	0,26	14.8936	1,6666	2
8	0.02222	0,26	14.8936	2,3333	1
9	0.02222	0,5	14.8936	2,3333	1
10	45,0725	0,26	14.8936	1	2
11	45,0725	0,5	14.8936	1	2
12	45,0725	0,5	14.8936	0.4286	2
13	45,0725	0,5	14.8936	1.6666	2
14	45,0725	0,5	14.8936	2.3333	1

Impact Factor:

ISRA (India) = 6.317
ISI (Dubai, UAE) = 1.582
GIF (Australia) = 0.564
JIF = 1.500

SIS (USA) = 0.912
PIHII (Russia) = 3.939
ESJI (KZ) = 8.771
SJIF (Morocco) = 7.184

ICV (Poland) = 6.630
PIF (India) = 1.940
IBI (India) = 4.260
OAJI (USA) = 0.350

References:

1. Lapin, Yu.V., & Strelets, M.X. (1980). *Vnutrennie techeniya gazovix smesey*. (p.368). Moscow: Nauka. Gl. red. Fiz - mat. Lit.
2. Rogov, B.V., & Sokolova, I.A. (2002). Obzor modeley vyazkix vnutrennix techeniy. *Matematicheskoe modelirovanie*, 2002, tom 14, № 1, pp. 41- 72.
3. Loytsyanskiy, L. G. (2003). *Mexanika jidkosti i gaza*. (p.840). Moscow: Drofa.
4. Slavkov, V. M. (1970). Smeshenie gazovix struy raznoy plotnosti. *Uchonie zapiski SAGI*. 1970, Tom 1, № 3, pp. 106-108.
5. Abramovich, G. N. (1991). *Prikladnaya gazovaya dinamika*. (p.600). Moscow: Nauka.
6. Vulis, L. A., & Kashkarov, V. P. (1965). *Teoriya struy vyazkoy jidkosti*. Moscow: Nauka.
7. Shishkin, N.E. (2015). Vliyanie visoti sheli i raznoy plotnosti koaksialnix struy na smeshenie v ogranichenom zakruchennom potoke. *Teplofizika i aeromexanika*. 2015, tom 22, № 4. pp. 445- 451.
8. Ferri, A. (1964). Supersonic combustion progress. «*Astronaut and Aeronaut*», 1964, № 8.
9. Craya, A., & Curtet, R. (1960). Riblications Scientifiques et Technolques du ministere de LAir , *Mars*, 1960, №359.
10. Barchilon, M., & Curtet, R. (1964). Trans. *ASME*, 1964, Ser. D. 4.
11. Baev, V.K., Konstantinovskiy, V.A., & Sidorov, I.V. (1972). Smeshenie sputnix potokov v kanale postoyannogo secheniya pri nalichii zoni retsirkulyatsii. *Fizika gorennya i vzriva*. 1972. № 1, pp. 70 - 76.
12. Bakaldina, L.A., & Sidorov, I.V. (1970). Usloviya sushestvovaniya i prodolnie razmeri retsirkulyatsionnix zon pri vzaimodeystvii sverxzvukovoy strui s ogranichenim sputnim dozvukovim potokom. *Izv. SO AN SSSR*, 1970. vip.2. № 8, pp. 37 - 45.
13. Vinogradov, Yu. V., Gruzdev, V.N., Postnov, V.F., & Talantov, A.V. (1977). Xarakteristika turbulentnosti pri techeniya sputnyx ploskix struy v zakrytom kanale. *Izv. AN SSSR. MJG*. 1977. № 2, pp. 175- 178.
14. Borisov, A.B., & Kovenya, V.M. (1976). Primenenie neyavnoy raznostnoy sxemi dlya rascheta vnutrennix techeniy vyazkogo gaza. V sb.: *Chisl. metodi mex. splosh. sredi*. Novosibirsk. 1976. T.7. № 4, pp. 36-47.
15. Fedotova, K.V., Arefeva, K.Yu., Suxov, A.V., & Yanovskiy, L.S. (2017). Issledovanie protsessov smesheniya produktov gazifikatsii tverdyx uglevodorodov s vysokoental'piynym gazovym potokom v kanalex postoyannogo secheniya. *Vestnik MGTU im. N.E. Baumana. Ser.Mashinostroenie*. 2017. № 4, pp. 11-27.
16. Birkin, A.P., Klyuev, V.N., Sosunov, A.Yu., & Tolstix, A.I. (1993). Chislennoe modelirovanie techeniya gaza v soplax Lavalya i techeniya tormojeniya v kanalex na osnove polnix uravneniy Navie- Stoksa. *Uchenie zapiski SAGI*. 1993. Tom XXIV. № 1, pp. 87- 97.
17. Lapin, Yu.V., Nexamkina, O.A., Pospelov, V.A., Strelets, M.X., & Shur, M.L. (1985). Chislennoe modelirovanie vnutrennix techeniy vyazkix ximicheski reagiruyushix gazovix smesey. *Itogi nauki i texniki. Ser. Mexanika jidkosti i gaza*. 1985, Moscow: Nauka, T.19. pp. 86 - 185.
18. Anderson, D., Tannexill, Dj., & Pletcher, R. (1990). *Vichislitel'naya gidromexanika i teploobmen*. V 2-x t. T. 2: Per.s angl. (pp.728, 392). Moscow: Mir.
19. Degi, D.V., & Starchenko, A.B. (2012). Chislennoe reshenie uravneniy Nav'e - Stoksa na kompyuterax s parallelnoy arxitekturoy. *Vestnik Tomskogo gosudarstvennogo universiteta. Matematika i mexanika*. 2012, № 2 (18).
20. Berezin, Yu.A., Kovenya, V.M., & Yanenko, N.N. (1972). Ob odnoy neyavnoy sxeme rascheta techeniya vyazkogo teploprovodnogo gaza. V sb. «*Chislennye metodi mexaniki sploshnoy sredi*», Novosibirsk. 1972.T.3. №4, pp. 3 - 18.
21. Kovenya, V.M., & Yanenko, N.N. (1981). *Metod rasshepleniya v zadachax gazovoy dinamiki*. (p.295). Novosibirsk: Nauka.
22. Xodjiev, S., & Pospelov, V.A. (1990). Primenenie sxemi Bima - Uorminga dlya rascheta techeniya v soplax Lavalya. V sb. *nauch. trud. «Gidroaerodinamika»*. Len. Gos. Tex. Uni, L.: 1990, pp.101 - 107.
23. Bim, R.M., & Uorming, R.F. (1978). Neyavnaya faktorizovannaya raznostnaya sxema dlya uravneniy Navie - Stoksa techeniya sjimaemogo gaza. *Raketnaya texnika i kosmonavtika*. 1978. t.16. №4, pp.145 - 156.